

See discussions, stats, and author profiles for this publication at: <https://www.researchgate.net/publication/7706345>

# P-Protein of Chandipura Virus Is an N-Protein-Specific Chaperone That Acts at the Nucleation Stage †

ARTICLE *in* BIOCHEMISTRY · APRIL 2004

Impact Factor: 3.02 · DOI: 10.1021/bi035793r · Source: PubMed

---

CITATIONS

17

---

READS

15

6 AUTHORS, INCLUDING:



**Soumen Basak**

National Institute of Immunology

21 PUBLICATIONS 865 CITATIONS

SEE PROFILE



**Dhruvajyoti Chattopadhyay**

Amity University, Kolkata

113 PUBLICATIONS 1,250 CITATIONS

SEE PROFILE



**Siddhartha Roy**

Bose Institute

146 PUBLICATIONS 2,625 CITATIONS

SEE PROFILE

# P-Protein of Chandipura Virus Is an N-Protein-Specific Chaperone That Acts at the Nucleation Stage<sup>†</sup>

Amitabha Majumdar,<sup>‡</sup> Raja Bhattacharya,<sup>‡</sup> Soumen Basak,<sup>‡</sup> M. S. Shaila,<sup>§</sup> Dhrubajyoti Chattopadhyay,<sup>\*,‡</sup> and Siddhartha Roy<sup>\*,||</sup>

*Dr. B. C. Guha Centre for Genetic Engineering and Biotechnology, Department of Biochemistry, University College of Science, University of Calcutta, 35 Ballygunge Circular Road, Calcutta 700 019, India, Department of Microbiology and Cell Biology, Indian Institute of Science, Bangalore 560 012, India, and Department of Biophysics, Bose Institute, P 1/12 CIT Scheme VII M, Calcutta 700 054, India*

*Received October 3, 2003; Revised Manuscript Received January 3, 2004*

**ABSTRACT:** The nucleocapsid protein N of Chandipura virus is prone to aggregation in vitro. We have shown that this aggregation occurs in two phases in a nucleation-dependent manner. Electron microscopy suggests that the aggregated state may have a ring-like structure. Using a GFP fusion, we have shown that the N-protein also aggregates in vivo. The P-protein suppresses the N-protein aggregation efficiently, both in vitro and in vivo. Increased lag phase in the presence of the P-protein suggests that chaperone-like action of the P-protein occurs before the nucleation event. The P-protein, however, does not exert any chaperone-like action against other proteins, suggesting that it binds to the N-protein specifically. Surface plasmon resonance and fluorescence enhancement indeed suggest that the P-protein binds tightly to the native N-protein. The P-protein is thus an N-protein-specific chaperone which inhibits the nucleation phase of N-protein aggregation, thus keeping a pool of encapsidation-competent N-protein for viral maturation.

Chandipura virus, a negative-stranded RNA virus, belongs to the vesicular stomatitis virus family (1). In this group of viruses, the RNA genome and the N-protein are folded together into a regular repeating structure, a “nucleocapsid”. Free N-proteins have a tendency to form large aggregates that are biologically inactive, and a cellular mechanism must exist to keep the protein soluble and functional (2, 3). Previously, it has been shown that the bacterially expressed unphosphorylated P-protein can suppress the aggregation of the N-protein (4, 5), but the mechanism of N-protein aggregation and its suppression by the P-protein is largely unknown. Also, the P-protein is present largely in a phosphorylated state in infected cells, in isolated virions, and in transfected cells expressing the P-protein gene (6). Thus, it is also important to study the properties of phosphorylated P-protein with respect to chaperone action.

It is increasingly becoming clear that many proteins may act as chaperones toward specific proteins, thus preventing aggregation. AHSP/hemoglobin, Hsc66/IscU, and hsp47/procollagen (7–9) are some of the important examples. Since P-protein has no obvious similarity to general chaperone proteins, it is possible that it exerts narrow substrate

specificity. Thus, an understanding of the mechanism of chaperone action of the P-protein and its substrate specificity is not only crucial for a molecular understanding of the life cycles of rhabdoviruses but the results may have implications for a general understanding of the protein-specific chaperones. In addition, it may provide us with a point to interfere with the viral life cycle for therapeutic purposes. In this paper we have explored the mechanism of how the phosphorylated P-protein prevents the aggregation of the N-protein.

## EXPERIMENTAL PROCEDURES

**Materials.** All polymerase chain reaction primers, dithiothreitol, Taq DNA polymerase, and T4 DNA ligase were from Genei (Bangalore, India). The gel extraction kit was from QIAGEN (Strassel, Germany). The CM5 sensor chip for BIACORE, the Mono-Q column for FPLC, *N*-hydroxysuccinimide ester, and EDC were from Amersham Pharmacia Biotech (Uppsala, Sweden). Alkaline phosphatase conjugated goat anti-mouse IgG was from Sigma. *N*-[1-(2,3-Dioleoyloxy)propyl]-*N,N,N*-trimethylammonium methyl sulfate, CKII,<sup>1</sup> and isopropyl thiogalactoside were from Roche Molecular Biochemicals (Mannheim, Germany). ATP was from Promega (Madison, WI). Fluorescein maleimide was from Molecular Probes Inc. (Eugene, OR). Prestained molecular mass markers and Bio-Beads SM2 adsorbent were from Bio-Rad (Hercules, CA). The pPEGFP vector was from Clontech (Palo Alto, CA). Dulbecco's modified Eagle's medium was from Gibco-BRL (Gaithersburg, MD). Triton-X-100 was

<sup>†</sup> We thank UGC, Calcutta University, for providing SRF to A.M., CSIR for providing SRF to S.B. and R.B., and DST for financial support.

<sup>\*</sup> To whom correspondence should be addressed. S.R.: tel, 91-33-2355-0254; fax, 91-33-2334-3886; e-mail, siddarth@boseinst.ernet.in and sidroy@vsnl.com. D.C.: fax, 91-33-2476-4419; e-mail, d\_jc@sify.com.

<sup>‡</sup> University of Calcutta.

<sup>§</sup> Indian Institute of Science.

<sup>||</sup> Bose Institute.

<sup>1</sup> Abbreviations: GFP, green fluorescent protein; CKII, casein kinase II; P0, nonphosphorylated P-protein; P1, monophosphorylated P-protein.

from Sigma Chemical Co. (St. Louis, MO) All other common reagents were of analytical grade.

**Protein Purification.** The P-protein of Chandipura virus was expressed in soluble form and was purified as described earlier (10). The N-protein of Chandipura virus was expressed in soluble form and was purified as described earlier (4). RNA content of the purified N-protein was measured by two methods: absorbance ratio and phenol extraction followed by alcohol precipitation. Both methods indicated only minor RNA contamination. The hydrated radius of the purified N-protein was also estimated by dynamic light scattering. The obtained value of about 30 Å indicates a monomeric species.

**Phosphorylation of P-Protein.** The purified unphosphorylated P-protein was phosphorylated in vitro by human recombinant CKII in 20 mM MES, pH 6.9, containing 130 mM KCl, 1 mM MgCl<sub>2</sub>, 100 μM ATP, and 1 mM DTT. The phosphorylation reaction was carried out at 37 °C for 2 h. After the reaction the protein was dialyzed against 50 mM Tris-HCl, pH 8.0, containing 150 mM NaCl for 4 h with three changes.

**Chemical Modification.** Phosphorylated P-protein (10 μM) was taken in 50 mM potassium phosphate buffer, pH 7.9, with a 20-fold molar excess of fluorescein maleimide (added as DMF solution in such a way that the final DMF concentration did not exceed 1%) and incubated at 4 °C for 30 min. During the incubation period the protein solution was constantly stirred, and after the incubation period it was shifted to 25 °C and kept for another 15 min. The reaction was quenched by 1 mM β-ME and dialyzed extensively against 50 mM Tris-HCl, pH 8.0, containing 150 mM NaCl. Using an extinction coefficient of 83000 M<sup>-1</sup> cm<sup>-1</sup> it was observed that 1.45 Cys residues in P1 could be labeled with fluorescein maleimide.

**Surface Plasmon Resonance.** All surface plasmon resonance studies were carried out in a BIAcore 2000 instrument (BIAcore) at 25 °C using HBS plus 0.005% surfactant P20 as flow buffer. For interaction studies the N-protein was taken in 10 mM sodium acetate, pH 4.2, and was cross-linked to a CM5 biosensor chip. The cross-linking was accomplished by first activating the surface with a 7 min pulse of *N*-hydroxysuccinimide ester/water-soluble carbodiimide mixture (30 μL at 5 μL/min) followed by a 6 min pulse of Chandipura N-protein (3 mg/mL in 10 mM sodium acetate, pH = 4.2), which was then injected over the CM5 chip after activation. After this, the chip was deactivated by a 6 min pulse of ethanolamine. Extensive washing with the flow buffer followed this process, and at the end there was about 1000 RUs of immobilization on the CM5 chip. The interaction was monitored in 50 mM Tris-HCl, pH 8.0, containing 150 mM NaCl so before doing the actual interaction the chip was primed with the buffer containing 50 mM Tris-HCl, pH 8.0, containing 150 mM NaCl. After priming P0 and P1 were passed as analytes over the sensor chip at a slow flow rate of 5 μL/min, the data were collected, and the resulting sensorgrams were analyzed.

**Electron Microscopy of Chandipura N-Nucleocapsids.** Chandipura N-protein was expressed and purified in soluble form from bacteria. From the purified protein, Triton X-100 was removed using Bio-Beads, and the protein was layered over 10 mL of 30% (v/v) glycerol in 20 mM Tris-HCl, pH 7.4, containing 150 mM NaCl. This was then centrifuged at

39000 rpm in a Beckman SW41 rotor for 18 h at 11 °C. After centrifugation the pellet was resuspended in 20 mM Tris-HCl, pH 7.4, containing 150 mM NaCl and dialyzed overnight against the same buffer at 4 °C. The dialyzed sample was centrifuged at 13000 rpm for 15 min. Then 10 μL of this sample (0.4 mg/mL) was taken and was adsorbed on the clean side of carbon-coated grids and was stained with 2% phosphotungstate. After air-drying the samples were viewed in a JEOL 1200 EXII electron microscope.

**DNA Constructs, Cells, and Transfection.** To monitor the N-protein aggregation in vivo, the N and GFP fusion protein had to be made. To make this chimera, pUC19 NC was digested with *Bam*HI, and the N gene insert was subcloned in the pEGFP-C1 vector. All in vivo experiments were done in HeLa cells. HeLa cells were grown in Dulbecco's modified Eagle's medium supplemented with 10% FBS, at 37 °C and at 5% CO<sub>2</sub> atmosphere. For transfection cells were grown in 12 mm coverslips, and when the cells were about 70% confluent, transfection was done with *N*-[1-(2,3-dioleoyloxy)-propyl]-*N,N,N*-trimethylammonium methyl sulfate using the manufacturer's protocol. For each transfection about 5–7 μg of DNA was used. Six hours after transfection, the cells were washed with PBS and then incubated in complete medium for an additional 34 h. After this 34 h period cells were taken and washed with PBS and fixed with an acetone and methanol (70:30) mixture. After fixing the cells were washed with PBS and were taken for viewing under a Zeiss confocal laser scanning microscope. To study the N aggregation in the presence of P and P mutant, P and P mutant cloned in the PCMXPL2 vector were cotransfected with GFP-N, and GFP fluorescence was monitored in the same way as stated above. GFP was monitored using blue filter excitation and green filter emission.

**Fluorescence Spectroscopy.** Steady-state fluorescence spectra were recorded in a Hitachi F 3010 spectrofluorometer. The fluorescence experiments were carried out at 30 °C where the temperature was maintained by a circulating water bath attached to the spectrofluorometer. The band-passes of excitation and emission were maintained at 5 nm, and all readings were taken in a cuvette of 1 cm path length. The fluorescence experiment for the N and fluorescein maleimide labeled P1 interaction was performed in 50 mM Tris-HCl, pH 8, containing 150 mM NaCl. Excitation and emission wavelengths were 480 and 520 nm, respectively. Anisotropy experiments were performed using a Hitachi polarization accessory.

**Static Light Scattering.** Chandipura N-protein at a high concentration was Millipore filtered three times and was added to a Millipore-filtered buffer under suitable dust-free conditions to a final protein concentration of 2 μM. All additions were made in the cuvette, and light scattering was measured with excitation and emission wavelengths set at 340 nm. All scattering intensities were measured at the same N-protein concentration with varying P-protein concentrations, and the scattering due to the buffer was subtracted from each value. Static light scattering experiments were done in 50 mM Tris-HCl, pH 8, containing 150 mM NaCl. Excitation and emission wavelengths were both 340 nm and band-passes were 5 nm for each. Aggregation of alcohol dehydrogenase/malate dehydrogenase was measured at 48 °C as an apparent optical density at A<sub>360</sub> using a Shimadzu UV160 spectrophotometer. The reaction was carried out in

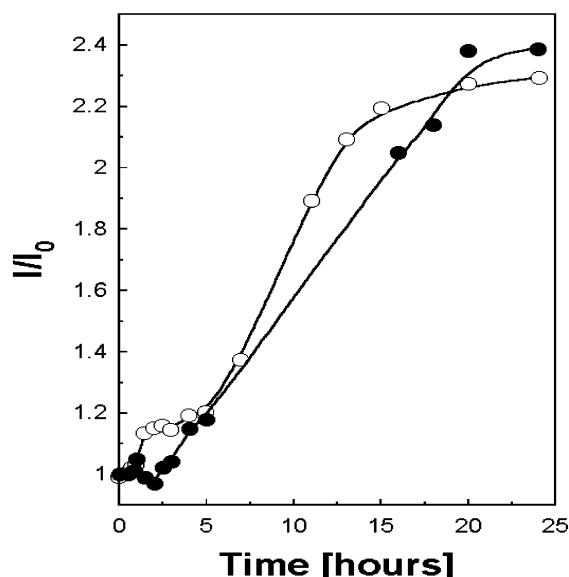


FIGURE 1: Aggregation kinetics of N-protein using static light scattering. The aggregation kinetics of varying concentrations of N-protein was monitored using static light scattering after removal of Triton X-100 from the N-protein using SM2 Bio-Beads. For each experiment N-protein was diluted from a concentrated stock to final concentrations of 12  $\mu$ M (open circle) and 6  $\mu$ M (solid circle), respectively, and Triton-X-100 was removed. The detergent-removed N-protein was taken in 50 mM Tris-HCl buffer, pH 8.0, containing 150 mM NaCl, and aggregation was monitored for a period of 24 h. The lines are trend lines and have no special significance.

100 mM sodium phosphate, pH 7, containing 0.1 M NaCl, and the readings of optical density were taken after every 100 s. For each aggregation experiment 6  $\mu$ M alcohol dehydrogenase or malate dehydrogenase was taken, and a 12  $\mu$ M concentration of P1 was taken. Insulin was dissolved in a minimum volume of 0.02 M NaOH, and for the experiment it was diluted to a concentration of 0.3 mg/mL with 100 mM sodium phosphate, pH 7. The reduction of insulin was initiated by adding 20  $\mu$ L of 1 M DTT to 1 mL of the sample in the cuvette. The extent of aggregation of the insulin B chain was measured as a function of time at 25 °C by monitoring light scattering at an excitation and emission of 360 nm. Excitation and emission band-passes were 1.5 nm using a Hitachi fluorometer.

**N-Protein Aggregation and Seeding Experiments.** The aggregation kinetics of N-protein was monitored using static light scattering after removal of Triton X-100 from the N-protein using SM2 Bio-Beads. N-Protein aggregation was monitored for two different final concentrations of detergent-removed N-protein, and they were 12 and 6  $\mu$ M. For seeding experiments the same aggregation kinetics of 6  $\mu$ M detergent-removed N-protein was monitored in the presence of a preformed seed of concentrations 0.6, 0.06, and 0.006  $\mu$ M, respectively. The seed was generated from a concentrated stock of detergent-removed N-protein, which has already reached the saturation of aggregation. The aggregation kinetics of N-protein in the presence and absence of seed was monitored using static light scattering for a period of over 24 h.

**Dynamic Light Scattering.** Dynamic light scattering experiments were performed using a DLS 700 instrument of Otsuka Electronics, Japan. For each of the experiments the sample was illuminated with a 638.8 helium–neon solid-

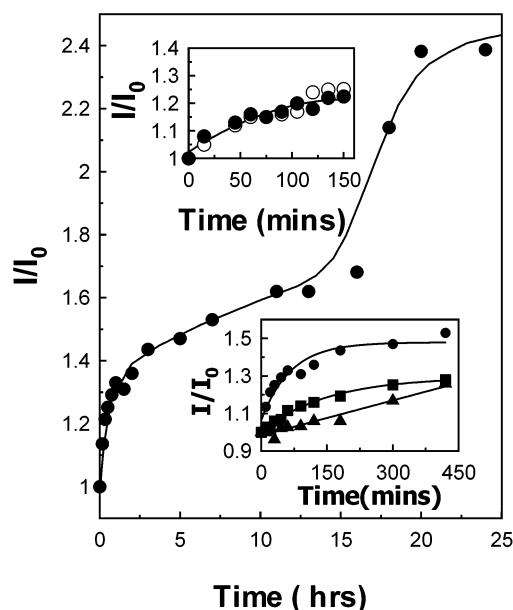


FIGURE 2: Seeding of N-protein aggregation with preformed aggregates. For the experiment concentrated stock of N-protein was taken, and Triton X-100 was removed using SM2 Bio-Beads. The detergent-removed N-protein was diluted to a concentration of 6  $\mu$ M and was taken in 50 mM Tris-HCl, pH 8.0, containing 150 mM NaCl, and to it preformed seed was added to a final concentration of 0.06  $\mu$ M. Seed was generated from a concentrated stock of detergent-removed N-protein, which has already reached the saturation of aggregation. The aggregation kinetics of N-protein in the presence and absence of seed was monitored using static light scattering for a period of over 24 h. The lower inset shows the effect of seed concentration on the first phase of N-protein aggregation. The seed was varied from a final concentration, in terms of monomer, of 0.006  $\mu$ M (solid triangle), 0.06  $\mu$ M (solid square), and 0.6  $\mu$ M (solid diamonds) and was added to a reaction containing 6  $\mu$ M detergent-removed N-protein in 50 mM Tris-HCl buffer, pH 8.0, containing 150 mM NaCl. The aggregation kinetics of N-protein in varying concentrations of seed was monitored using static light scattering for a period of over 24 h. The upper inset shows the effect of P-protein on the seeded aggregation reaction of the N-protein. Aggregation kinetics of N-protein (6  $\mu$ M) was monitored in the presence of 0.6  $\mu$ M N-protein seed in the presence (solid circle) and absence of 6  $\mu$ M P-protein (open circle).

state laser, and the intensity of light scattered at an angle of 90° was measured. An autocorrelation function was used to determine the translational diffusion coefficient ( $D_T$ ) of the sample particles in the solution by measuring the fluctuations in the intensity of the scattered light. The hydrodynamic radius ( $R_H$ ) of the sample particles was derived from  $D_T$  using the Stokes–Einstein equation

$$D_T = k_b T / 6 \pi \eta R_H$$

where  $k_b$  is the Boltzman constant,  $T$  is the absolute temperature in degrees kelvin, and  $\eta$  is the solvent viscosity. For each experiment 6  $\mu$ M N-protein was taken, and P1 was taken accordingly. All experiments were done in 50 mM Tris-HCl, pH 8, containing 150 mM NaCl.

**Interaction of RNA with Aggregated N-Protein (Bio-Beads Treated) GEMSA.** The leader RNA probe was incubated in binding buffer (same as above) for 15 min at 37 °C in a total reaction volume of 20  $\mu$ L with 400 ng/ $\mu$ L soluble recombinant N-protein (in the presence of 0.1% Triton X 100) or with N-protein treated with Bio-Beads (Bio-Rad) and allowed to aggregate for different time spans (0, 1, 3,



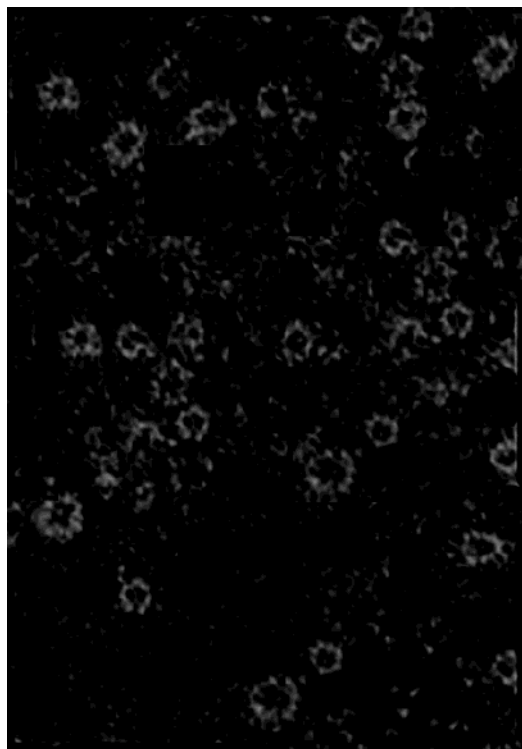


FIGURE 3: Transmission electron microscopy of N aggregates. Triton X-100 was removed using Bio-Beads, and the protein was processed as described in Experimental Procedures. The samples were observed under an electron microscope after being negatively stained with 2% potassium phosphotungstate. The images were viewed with 80000 $\times$  magnification.

and 24 h). Native gel loading dye was added to the reaction mixture, and the complexes were resolved on a 4% native polyacrylamide gel containing 5% glycerol, run at 4  $^{\circ}$ C in 1 $\times$  TAE. The gel was dried and exposed to X-ray film.

## RESULTS AND DISCUSSION

The protein aggregation mechanism can be complex, but the study of aggregation kinetics can reveal significant details about the assembly pathway. Previously, we have shown that the free N-protein is prone to aggregation and the P-protein is able to suppress this aggregation. The mechanism of suppression of aggregation is, however, largely unknown. Figure 1 shows the kinetics of aggregation at two different N-protein concentrations (6 and 12  $\mu$ M). The aggregation kinetics at 6  $\mu$ M suggests the presence of a lag phase, which is a characteristic of a nucleation-dependent aggregation process. The lag phase is significantly reduced at the 12  $\mu$ M concentration, supporting the existence of a nucleation event. Interestingly, at the higher protein concentration, the aggregation kinetics appears biphasic.

Seeding is often used to enhance the nucleation step. Figure 2 shows the kinetics of aggregation of the N-protein in the presence of added seed. It is clear that addition of the seed dramatically reduces the lag phase in a concentration-dependent manner (lower inset). It is also clear that the aggregation kinetics is biphasic in nature and the second phase may have a separate lag phase, which is not pronouncedly affected by the presence of the seed. It appears that initially a structure is assembled in a nucleation-dependent manner, which then assembles into a higher order structure, also in a nucleation-dependent manner. The action

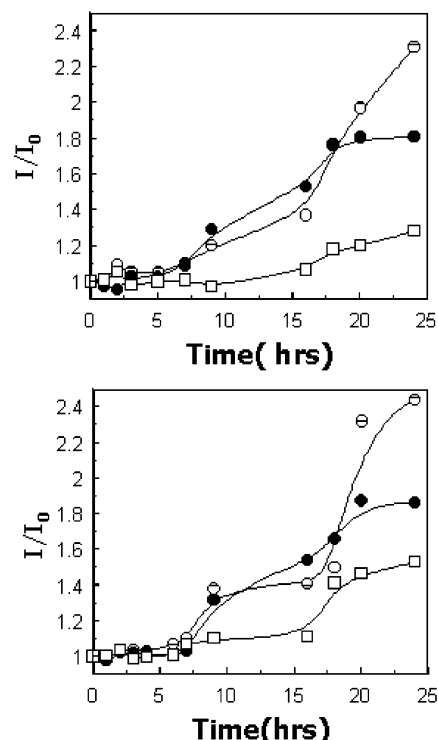


FIGURE 4: Aggregation kinetics of N-protein in the presence and absence of varying concentrations of P1 (upper panel) and P0 (lower panel) using static light scattering. The N-protein aggregation kinetics was monitored using static light scattering in the presence and in absence of varying concentrations of P1 and P0. For each experiment 6  $\mu$ M Triton X-100-removed N-protein was taken, and P1 and P0 were taken in three different concentrations of 3  $\mu$ M (open circle), 6  $\mu$ M (solid circle), and 9  $\mu$ M (open square). All experiments were done in 50 mM Tris-HCl buffer, pH 8.0, containing 150 mM NaCl.

of the P-protein in the nucleation stage was confirmed by observing the effect of P-protein on the seeded aggregation reaction. If the P-protein does not inhibit the seeded reaction, it is a proof of its action at the nucleation stage. The upper inset shows the effect of P-protein on the seeded reaction. No significant effect is seen, indicating that the P-protein acts at the nucleation stage.

We have attempted to elucidate the possible nature of the aggregate by electron microscopy. For this experiment N-protein was expressed and purified in a soluble form, followed by aggregation *in vitro*. From the electron microscope images, it is clear that the N-protein forms a ring-like aggregated structure of diameter  $210 \pm 5$   $\text{\AA}$  (Figure 3). In some cases, these individual ring structures were heaped upon one another. We conclude that formation of the rings is an important part of the aggregation process. Whether the rings are the intermediate or final products is not known. However, given the biphasic kinetics, it is tempting to speculate that the intermediate species are the rings and the assembly of the rings produce the higher order structure.

**Chaperone Action of Phosphorylated P-Protein.** Our previous work has established that bacterially expressed P is unphosphorylated and suppresses N-protein aggregation (4). P-Protein remains mostly in a phosphorylated state when it is isolated from virion or infected cells or from cells where P-protein is expressed alone (11). To assess the chaperone potential of the phosphorylated P-protein, the N-protein aggregation kinetics was monitored using static light scat-

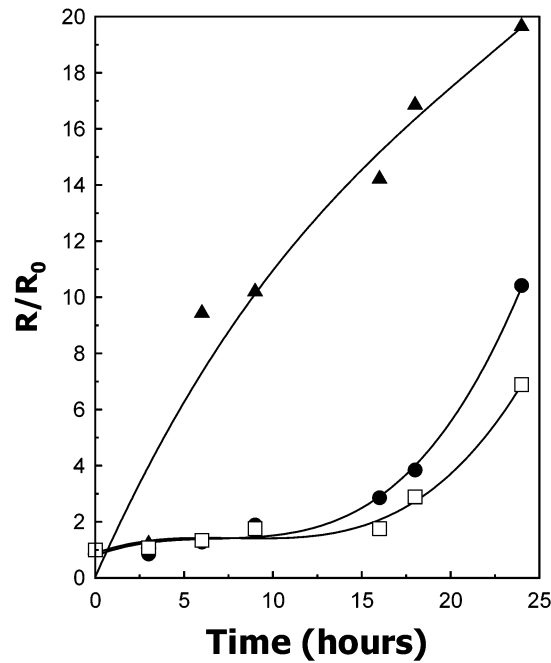


FIGURE 5: Aggregation kinetics of N-protein in the presence and absence of varying concentrations of P0 and P1 using dynamic light scattering. The N-protein aggregation kinetics was monitored using dynamic light scattering after removal of Triton X-100 from the N-protein using SM2 Bio-Beads. For each experiment 6  $\mu$ M Triton X-100-removed N-protein was taken, and P0 and P1 were taken accordingly. All experiments were done in 50 mM Tris-HCl buffer, pH 8.0, containing 150 mM NaCl. The solid triangles are for N-protein only, the open squares are for N:P0 (1:1.5), and the solid circles are for N:P1 (1:1.5).

Table 1: Chaperone Action of the Phosphorylated P-Protein during Refolding of N-Protein<sup>a</sup>

system	relative scattering intensity after 10 min
1 $\mu$ M N	602.6
1 $\mu$ M N + 0.25 $\mu$ M P1 (P0 + ATP + CKII)	313.9
1 $\mu$ M N + 0.5 $\mu$ M P1 (P0 + ATP + CKII)	261.7
1 $\mu$ M N + 1.0 $\mu$ M P1 (P0 + ATP + CKII)	240.9
1 $\mu$ M N + 2.0 $\mu$ M P1 (P0 + ATP + CKII)	187.6
1 $\mu$ M N + 4.0 $\mu$ M P1 (P0 + ATP + CKII)	167.2
1 $\mu$ M N + 0.5 $\mu$ M P0	382.4
1 $\mu$ M N + 0.25 $\mu$ M P0 (P0 + CKII + dATP)	552.8
1 $\mu$ M N + 0.25 $\mu$ M P0 (P0 + ATP)	568.8

<sup>a</sup> From a concentrated stock of N-protein, Triton X-100 was removed by Bio-Beads, denatured with 8 M urea, and allowed to refold in a native buffer. Aggregation during refolding was monitored in the presence of varying concentrations of the P-protein. The P-protein was phosphorylated by incubating P0 with ATP and CKII at 37 °C in 50 mM Tris-HCl buffer, pH 8.0, containing 150 mM NaCl. The phosphorylated P was then added to N prior to refolding and light scattering monitored. For line 7, instead of CKII and ATP, buffer was added, and hence there was no phosphorylation; for line 8, dATP was added instead of ATP, in which case there should be no phosphorylation. For line 9, no CKII is added, and hence there should be no phosphorylation either.

tering after removal of Triton X-100 from the N-protein. This aggregation kinetics was monitored in the absence and in the presence of varying concentrations of P1 and P0. The aggregation kinetics of N-protein after Triton X-100 removal has a substantial lag phase, suggesting a process of nucleation during this time. As shown in Figure 4, P1 and P0 both extend this lag phase substantially in a concentration-

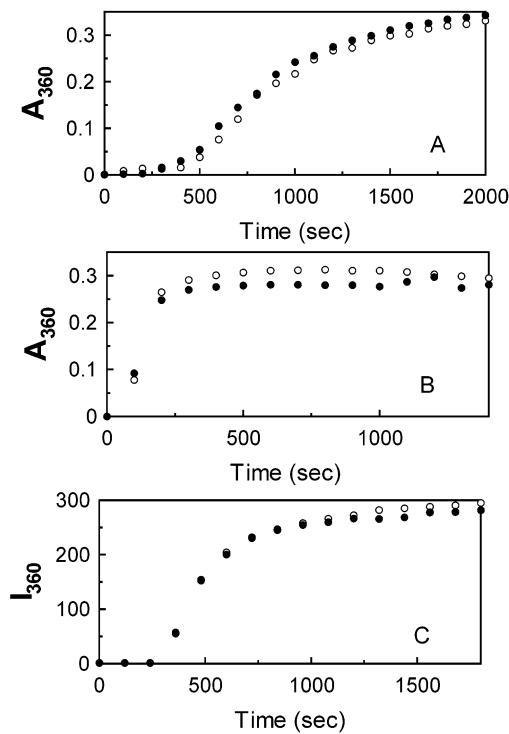


FIGURE 6: Effect of P1 on the kinetics of aggregation: (A) malate dehydrogenase, (B) alcohol dehydrogenase, and (C) insulin. Aggregation of alcohol dehydrogenase/malate dehydrogenase was measured at 48 °C by measuring absorbance at 360 nm using a Shimadzu UV160 spectrophotometer. The reaction was carried out in 100 mM sodium phosphate, pH 7, containing 0.1 M NaCl. For each aggregation experiment 6  $\mu$ M alcohol dehydrogenase or malate dehydrogenase was taken, and a 12  $\mu$ M concentration of P1 was taken. DTT-induced insulin aggregation was measured in a fluorometer at 0.3 mg/mL in 100 mM sodium phosphate, pH 7 at 25 °C. Excitation and emission wavelengths were set at 360 nm, and the band-passes were 1.5 nm. The filled circles are with P1, and the open circles are without P1.

dependent manner, suggesting that at least it partially delays the nucleation process. To substantiate the kinetic data obtained from static light scattering, the same experiment of N-protein aggregation was monitored using dynamic light scattering. Here the Triton -X-100-removed N-protein was taken, and the aggregation was monitored by following the increase of the Stokes radius with time in the presence and absence of P1 (Figure 5). The effect of the same concentration of P0 was shown as a control. The results showed a similar pattern as the static light scattering experiment, and both P1 and P0 delayed the onset of aggregation and the size of the aggregate. The effect is also directly proportional to the concentration of P-protein (data not shown). However, P1 is not able to stop aggregation when added after 18 h of time. The effect is partial if added after 4 h of time (data not shown). Importantly, the relative scattering intensity does not decrease from the value at the time of P1 addition, indicating that P1 cannot dissolve the already formed aggregates.

Many chaperones also protect refolding proteins from aggregating. To find out if the phosphorylated P-protein could act like a chaperone toward N-protein during refolding process and prevent its aggregation, the urea-denatured N-protein was allowed to refold in a native buffer in the fluorometer cuvette, and aggregation during refolding was monitored using light scattering. The scattering values as a

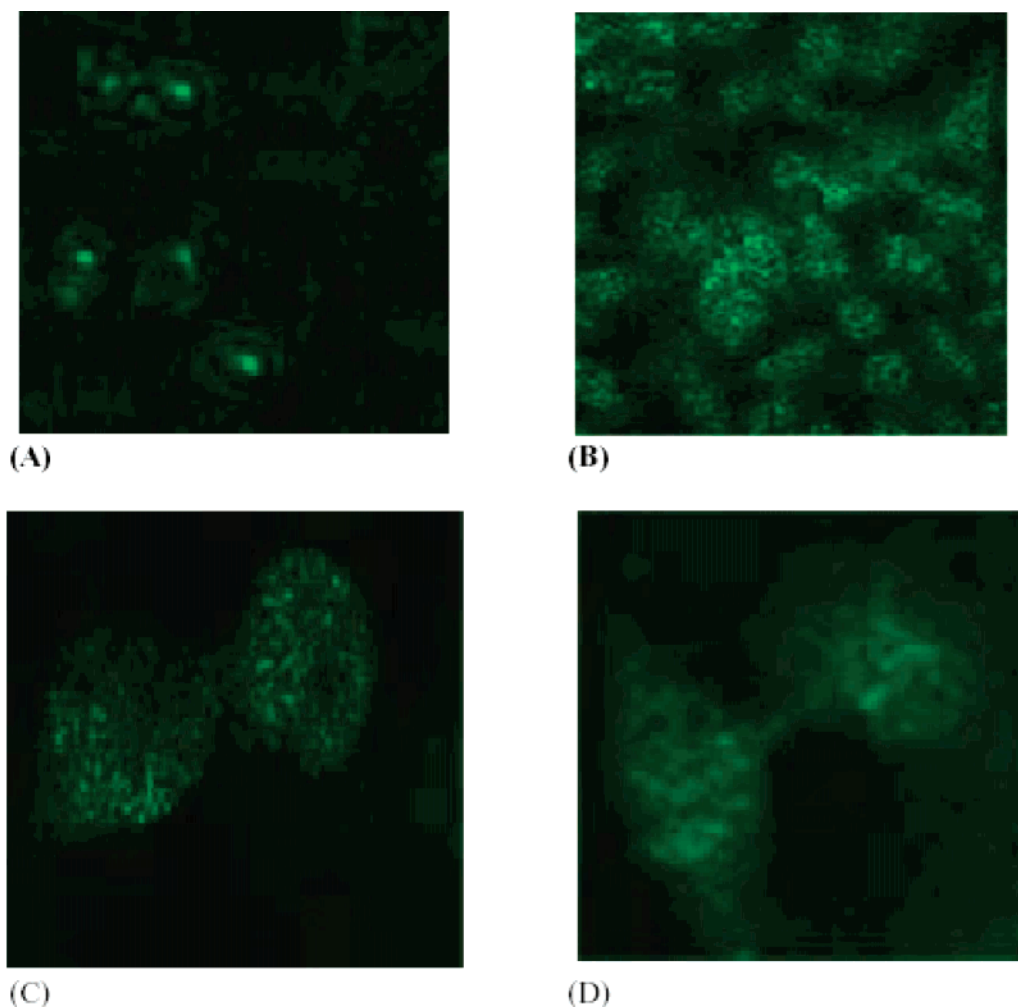


FIGURE 7: In vivo aggregation of N-protein and its suppression by P. (A) Fluorescence from the N-GFP construct. (B) GFP fluorescence from the vector. (C) P cotransfected with GFP-N. (D) Mutant P cotransfected with GFP-N. The N gene was subcloned in the pEGFP-C1 vector and was transfected to HeLa cells. Expression and distribution of N-GFP chimera were monitored 40 h after transfection. For coexpression experiments, the N-GFP construct was cotransfected with P and mutant P cloned in the PCMXPL2 vector, and distribution of GFP fluorescence was monitored using a confocal microscope 40 h after cotransfection.

function of time were relatively flat but much higher than protein alone controls (data not shown). This suggests that refolding and aggregation were over within the mixing dead time. Table 1 shows the light scattering after 10 min of initiation of refolding at different ratios of N and P1. Increasing concentrations of P1 suppress the aggregation of the N-protein, and the effect gradually saturates, indicating that the P1 has chaperone-like activity toward the N-protein. As a control, the effectiveness of unphosphorylated P-protein was compared. It appears from the results that P1 is somewhat better than P0 as a chaperone.

To determine if Chandipura P1 is a generalized chaperone or its action is specifically directed toward N, we measured if P1 can suppress the dithiothreitol-induced aggregation of insulin and heat-induced aggregation of malate dehydrogenase and alcohol dehydrogenase (12). It was observed that a high concentration of P1 could not suppress aggregation of any of these proteins (Figure 6). This suggests that P1 may be a specific chaperone toward N. Recently, several papers have appeared demonstrating the existence of protein-specific chaperones. Why the existing chaperone machinery in the cell is insufficient for these proteins is not known. One possibility is that aggregation of some proteins may occur from states that are close to native. The existing

chaperone machinery probably in most cases binds relatively hydrophobic epitopes, which are characteristics of denatured states. Thus, protein-specific chaperones may have evolved to bind epitopes on native or nativelike states.

One of the ways to study protein aggregation in vivo is to fuse the protein of interest with GFP, express the fusion protein in cells, and monitor the distribution of GFP fluorescence (13). If the protein aggregates in vivo, then most of the GFP-N-protein would coalesce and GFP fluorescence would originate from one or two regions in the cells (14). The CHP-N gene was cloned in the pEGFPC1 vector to produce the GFP-N fusion protein, the GFP-N clone was transfected to HeLa cells along with a vector control, and the GFP fluorescence was monitored at 40 h after transfection. In about 85% of GFP-N transfected cells the intense GFP fluorescence emanated from one or two regions in the cells, and there was very little background fluorescence indicating aggregated protein (Figure 7A). In contrast, in the vector control the GFP fluorescence was distributed throughout the cell (Figure 7B). In vivo protein aggregation can be suppressed if chaperones are coexpressed with proteins that have an aggregating tendency (14). The transfection experiment mentioned above was performed with cotransfection of the P gene or a phosphorylation-defective mutant with

GFP-N and GFP fluorescence monitored after 40 h. It could be seen that both P and phosphorylated P disperse the fluorescence of the GFP-N fusion protein, indicating that both can suppress N aggregation *in vivo* (Figure 7C,D). About 70% of the cells in GFP-N + P and GFP-N + mutant P transfected cells showed distribution of GFP fluorescence like the vector only control. The PCMXPL2 vector (in which the P-protein was cloned) transfection showed no effect on GFP-N aggregation (data not shown).

**Interaction of the P-Protein with the N-Protein.** Experiments described above have shown that bacterially expressed and CKII-phosphorylated P-protein (P1) can act like a chaperone and can suppress N aggregation. If P1 exerts chaperone-like activity toward N, then N and P1 must show specific interaction. Previously, using fluorescently labeled P0 we have shown that N-protein and P0 can interact (4). But using the same strategy we could not detect specific N–P1 interaction, so we tried monitoring the N–P1 interaction using surface plasmon resonance (15). For this purpose N-protein was immobilized directly on a CM5 sensor chip, P1 was injected at varying concentrations, the interaction was monitored using the BIAcore system, and the sensorgrams were detected. The sensorgrams of the resonance units versus time showed that N–P1 interaction has a good on-rate, which indicated complex formation, but the off-rate is very fast (Figure 8, upper panel). Although it is difficult to accurately determine the dissociation constant from these data, an approximate upper limit of around  $10^{-5}$  M can be estimated. The surface plasmon resonance experiment qualitatively established that N and P1 interacted. To further substantiate this fact, N and P1 interaction was monitored using fluorescence spectroscopy. For this purpose fluorescein maleimide labeled P1 was used as the probe and was titrated with varying concentrations of CHP-N-protein. Figure 8 (lower panel) shows the fluorescence enhancement as a function of increasing concentrations of N-protein. The enhancement of fluorescence saturated quickly, suggesting a specific complex formation. The fluorescence increase can be fitted to a binding equation with a dissociation constant of  $9.6 \times 10^{-7}$  M. This is consistent with the upper limit derived from SPR experiments. From the previous experiments it is quite clear that P1 can inhibit the aggregation of N-protein and N–P1 interact to form a specific complex. We hypothesize that the P-protein has evolved to specifically bind N-protein and the complex cannot form aggregates due to steric and other reasons. The highly charged N-terminal arm of the P-protein helps to solubilize the N–P complex, thus exerting specific chaperone action. An interesting aspect of N–P interaction is that apparently the N–P0 and N–P1 interaction appears to be different. Whereas N–P0 complex formation leads to fluorescence increase of a labeled N, little or no fluorescence increase was observed with the same labeled N-protein upon N–P1 complex formation. How the two complexes differ, if at all, and its possible biological role remain to be investigated.

Major biological role of nucleocapsid protein is to bind with viral genome and encapsidate it in an RNase-resistant form. Removal of Triton X-100 using Bio-Beads renders the soluble N-protein to form aggregates in a time-dependent manner as evident from the light scattering experiments. The ability of these protein aggregates to bind and encapsidate the RNA probe was monitored through gel shift assay. The

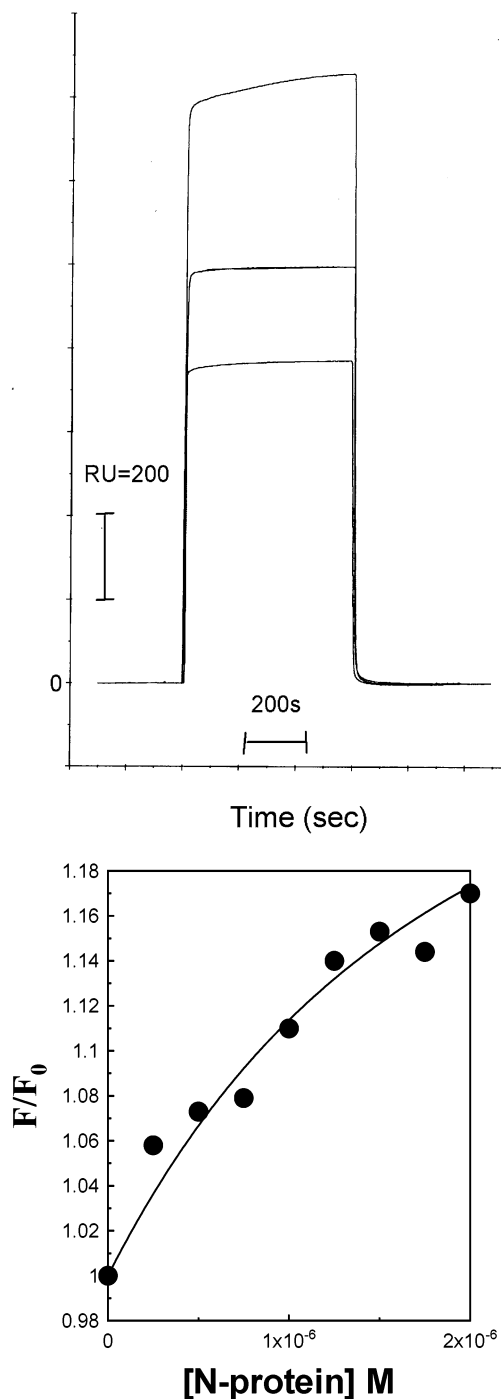


FIGURE 8: Interaction of N-protein with P1 (upper panel) using surface plasmon resonance and (lower panel) using fluorescence spectroscopy. For surface plasmon resonance measurements, N-protein was cross-linked to a CM5 biosensor chip as described in Experimental Procedures. P1 was then passed as analyte over the sensor chip at a slow flow rate of  $5 \mu\text{L}/\text{min}$ , the data were collected, and the resulting sensorgrams were analyzed. The P1 concentrations are 2, 3, and  $4 \mu\text{M}$  from the bottom. The fluorescence experiment with N and fluorescein maleimide labeled P1 ( $0.5 \mu\text{M}$ ) was performed in  $50 \text{ mM}$  Tris-HCl, pH 8, containing  $150 \text{ mM}$  NaCl at  $37^\circ\text{C}$ . Excitation and emission wavelengths were 480 and 520 nm, respectively.

binding started to decrease from the very onset of Bio-Beads treatment (1 h time point) as compared to the complex formed by an equal amount of treated N-protein control (0 h time point). This trend of decrease in binding and encapsidation continued with increasing the time of aggrega-



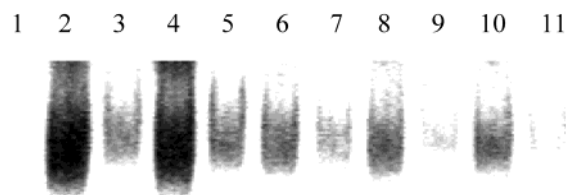


FIGURE 9: Encapsidation of the leader RNA probe by N-protein as a function of time after Bio-Beads treatment. Lanes: 1, free RNA; 2 and 3, RNase untreated and treated 0 h control without Bio-Beads treatment, respectively; 4 and 5, RNase untreated and treated 0 h Bio-Beads treated complex, respectively; 6 and 7, RNase untreated and treated 1 h Bio-Beads treated complex, respectively; 8 and 9, RNase untreated and treated 3 h Bio-Beads treated complex, respectively; 10 and 11, RNase untreated and treated 24 h Bio-Beads treated complex, respectively. The leader RNA probe was incubated in binding buffer for 15 min at 37 °C in a total reaction volume of 20  $\mu$ L with 400 ng/ $\mu$ L soluble recombinant N-protein (in the presence of 0.1% Triton X-100) or with N-protein treated with Bio-Beads (Bio-Rad) allowing to aggregate for different time intervals (0 h, 1 h, 3 h, and 24 h).

tion until at the 24 h time point, where almost no binding was detectable. With time, the RNase sensitivity of the complex also increased, and from 3 h onward the complex started to disappear upon treatment with RNase (Figure 9). This suggests that the aggregated N-protein is incapable of proper encapsidation and P1 plays a vital role to keep it soluble and encapsidation competent.

Encapsidation of viral genomes is a complex process. It appears that most capsid proteins are flexible in nature. This flexibility is perhaps the result of a requirement of conformational changes during the process of encapsidation. Nucleic acid binding proteins that have broad sequence specificity are known to possess flexibility. The downside of having a highly flexible protein is that they are prone to aggregation as some of the internal hydrophobic patches become exposed easily. The nucleocapsid protein, N, of Chandipura virus is no exception. In a previous study we have shown that the Chandipura N-protein has significant internal flexibility and propensity toward aggregation in vitro. Since a relatively large amount of N-protein is produced during the viral life cycle, aggregation and encapsidation must compete. Different viruses have probably evolved different mechanisms to cope with this necessary evil of flexibility. Vesicular stomatitis virus and related viruses may have evolved N-specific chaperone activity in phosphoprotein

P that suppresses aggregation of N-protein, in vitro and in vivo. If indeed the epitope on N interacts specifically with P1, it may be possible to devise molecules that may block this interaction. Thus, this interaction may be a legitimate target for antiviral drug design.

## ACKNOWLEDGMENT

We gratefully acknowledge Prof. S. P. Maulik, Jadavpur University, for providing the facilities of dynamic light scattering. We thank Dr. Indi and Flora Martin, IISc Bangalore, for helping in the EM and surface plasmon resonance studies, respectively. We thank Mr. Sandipan Ganguly, NICED Kolkata, for helping in confocal studies. We thank Prof. B. Bhattacharyya, BI, for help with protein aggregation studies.

## REFERENCES

1. Bhatt, P. N., and Rodrigues, F. M. (1967) *Indian J. Med. Res.* 55, 1295–1305.
2. Masters, P. S., and Banerjee, A. K. (1988) *J. Virol.* 62, 2651–2657.
3. Masters, P. S., and Banerjee, A. K. (1988) *J. Virol.* 62, 2658–2664.
4. Majumder, A., Basak, S., Raha, T., Chowdhury, S. P., Chattopadhyay, D., and Roy, S. (2001) *J. Biol. Chem.* 276, 30948–30955.
5. Barik, S., and Banerjee, A. K. (1992) *J. Virol.* 66, 1109–1118.
6. Masters, P. S., and Banerjee, A. K. (1986) *Virology* 154, 259–270.
7. Kihm, A. J., Kong, Y., Hong, W., Russell, J. E., Rouda, S., Adachi, K., Simon, M. C., Blobel, G. A., and Weiss, M. J. (2002 Jun 13) *Nature* 417, 758–763.
8. Hoff, K. G., Ta, D. T., Tapley, T. L., Silberg, J. J., and Vickery, L. E. (2002) *J. Biol. Chem.* 277, 27353–27359.
9. Tasab, M., Jenkinson, L., and Bulleid, N. J. (2002) *J. Biol. Chem.* 277, 35007–35012.
10. Raha, T., Chattopadhyay, D., Chattopadhyay, D., and Roy, S. (1999) *Biochemistry* 38, 2110–2116.
11. Barik, S., and Banerjee, A. K. (1992) *Proc. Natl. Acad. Sci. U.S.A.* 89, 6570–6574.
12. Manna, T., Sarkar, T., Poddar, A., Roychowdhury, M., Das, K. P., and Bhattacharyya, B. (2001) *J. Biol. Chem.* 276, 39742–39747.
13. Satyal, S. H., Schmidt, E., Kitagawa, K., Sondheimer, N., Lindquist, S., Kramer, J. M., and Morimoto, R. I. (2000) *Proc. Natl. Acad. Sci. U.S.A.* 97, 5750–5755.
14. Krobitsch, S., and Lindquist, S. (2000) *Proc. Natl. Acad. Sci. U.S.A.* 97, 1589–1594.
15. Kersh, G. J., Kersh, E. N., Fremont, D. H., and Allen, P. M. (1998) *Immunity* 9, 817–826.

BI035793R